International Journal of Pharmaceutics 619 (2022) 121691

Contents lists available at ScienceDirect

International Journal of Pharmaceutics

journal homepage: www.elsevier.com/locate/ijpharm

pH-temperature dual-sensitive nucleolipid-containing stealth liposomes anchored with PEGylated AuNPs for triggering delivery of doxorubicin

Mónica C. García [a,b,c,*], José Manuel Calderón-Montaño [d], Manuela Rueda [e], Marcela Longhi [a,b], Antonio M. Rabasco [c], Miguel López-Lázaro [d], Francisco Prieto-Dapena [e], María Luisa González-Rodríguez [c,*]

[a] Universidad Nacional de Córdoba, Facultad de Ciencias Químicas, Departamento de Ciencias Farmacéuticas, Ciudad Universitaria, Haya de la Torre and Medina Allende, Science Building 2, Córdoba X5000HUA, Argentina

[b] Consejo Nacional de Investigaciones Científicas y Técnicas, CONICET, Unidad de Investigación y Desarrollo en Tecnología Farmacéutica, UNITEFA, Córdoba X5000HUA, Argentina

[c] Department of Pharmacy and Pharmaceutical Technology, Faculty of Pharmacy, Universidad de Sevilla, C/Prof. García González 2, 41012 Seville, Spain

[d] Department of Pharmacology, Faculty of Pharmacy, Universidad de Sevilla, C/Prof. García González 2, 41012 Seville, Spain

[e] Department of Physical Chemistry, Faculty of Chemistry, Universidad de Sevilla, C/Prof. García González s/n, 41012 Seville, Spain

A R T I C L E I N F O

Keywords:
Thermo-responsive liposomes
pH-responsive liposomes
Drug delivery
Gold nanoparticles
Langmuir monolayers
Anticancer activity

A B S T R A C T

Liposomes (Lip) are useful nanocarriers for drug delivery and cancer nanomedicine because of their ability to efficiently encapsulate drugs with different physical and chemical properties. The pH gradient between normal and tumoral tissues, and their rapid metabolism that induces hyperthermia encourage the development of pH- and thermo-sensitive Lip for delivering anticancer drugs. Nucleolipids have been studied as scaffolding material to prepare Lip, mainly for cancer therapy. Herein, we report for the first time the use of 1,2-dipalmitoyl-*sn*-glycero-3-(cytidine diphosphate) (DG-CDP) to develop pH/thermo-sensitive nucleolipid-containing stealth Lip stabilized by combination with 1,2-dipalmitoyl-*sn*-glycero-3-phosphocholine (DPPC) and cholesterol, anchored with NH_2-PEGylated gold nanoparticles (PEG-AuNPs, 15 nm) for triggering delivery of doxorubicin (Dox). The optimal composition of DPPC, DG-CDP and cholesterol (94:3:3) was established by Langmuir isotherms. Unloaded and Dox-loaded Lip and AuNPs-Lip exhibited nano-scale sizes (415–650 nm), acceptable polydispersity indexes (<0.33), spherical shapes, and negative Z-potential (−23 to −6.6 mV) due to the phosphate groups of DG-CDP, which allowed the anchoring with positively charged AuNPs. High EE% were achieved (>78%) and although efficient control in the Dox release towards different receptor media was observed, the release of Dox from PEG-AuNPs-Lip-Dox was significantly triggered at acidic pH and hyperthermia conditions, demonstrating its responsiveness to both stimuli. Dox-loaded Lip showed high cytotoxic activity against MDA-MB-231 breast cancer cells and SK-OV-3 ovarian cancer cells, suggesting that Dox was released from these nanocarriers over time. Overall, the liposomal formulations showed promising properties as stimuli-responsive nanocarriers for cancer nanomedicine, with prospects for hyperthermia therapy.

1. Introduction

The use of nanostructures as multifunctional platforms for targeting drugs in order to increase their efficacy in the tissue to be treated and minimize the side effects in the rest of the organism is among the priorities of advanced therapeutic nanocarriers. With the advancement of research in the field of nanomedicine, a large number of drug delivery systems have been developed to date, including those based on lipids, polymers, inorganic components, etc. (García, 2019; García et al., 2017), and also hybrid systems combining them (García and Uberman, 2019; Milczewska et al., 2016).

Lipid vesicles, known as liposomes (Lip), were the first nanotechnology-based delivery systems reported by Bangham *et al.* in the 70s (Bangham and Horne, 1964). Since then, Lip have been widely

* Corresponding authors at: Haya de la Torre and Medina Allende, Science Building 2, Department of Pharmaceutical Sciences, Faculty of Chemical Sciences, National University of Cordoba, University City, X5000HUA Córdoba, Argentina (M.C. García). Department of Pharmacy and Pharmaceutical Technology, Faculty of Pharmacy, Universidad de Sevilla, C/Prof. García González 2, 41012 Seville, Spain (M.L. González-Rodríguez).

E-mail addresses: mgarcia@unc.edu.ar (M.C. García), malugoro@us.es (M.L. González-Rodríguez).

https://doi.org/10.1016/j.ijpharm.2022.121691
Received 8 October 2021; Received in revised form 5 March 2022; Accepted 18 March 2022
Available online 21 March 2022
0378-5173/© 2022 The Author(s). Published by Elsevier B.V. This is an open access article under the CC BY-NC-ND license (http://creativecommons.org/licenses/by-nc-nd/4.0/).

studied and have risen as one of the most useful tools for developing nanocarriers for drug delivery. These lipid systems provide numerous advantages due to their biomimicking cell membranes, capability to entrap hydrophilic and lipophilic molecules, biocompatibility and biodegradability, low immunogenicity and negligible toxicity, high chemical versatility, etc. (Large et al., 2021).

A major drawback of conventional Lip is that the mononuclear phagocyte system can recognize them after systemic administration, and subsequently, they can be quickly cleared by the reticuloendothelial system (Aghdam et al., 2019). Adsorption of proteins and corona formation are generally associated with the recognition of Lip, as well as other nanocarriers, by the immune system and their clearance from the systemic circulation. The most common strategy that has been used to reduce protein binding is the coating with inert biocompatible polymers, such as polyethylene glycol (PEG) on the surface of Lip to obtain the so-called 'stealth' surfaces (Franco et al., 2021). Furthermore, it has been demonstrated that incorporation of zwitterionic lipids in Lip, similar to PEGylation, allows reducing protein binding and increasing plasma residence time (Montizaan et al., 2020). Moreover, a great challenge facing drug delivery systems for cancer therapy is the liposomal trigger at the tumor site (Franco et al., 2021). In this regard, Lip can be designed to prevent or minimize drug release in the bloodstream and normal tissues and release their payload only when exposed to a specific trigger stimulus at the tumor site, obtaining optimal anticancer effects (Aghdam et al., 2019).

Normal tissues and other biological fluids have a pH value of ~7.4. The extracellular pH of tumors is ~6.5–7.2, and its value is even lower in intracellular endosomes (5.5–5.0) and lysosomes (4.0–4.5) (Boedtkjer and Pedersen, 2020; Franco et al., 2021; Koltai, 2020; Li et al., 2019; Torres et al., 2020). Taking advantage of this pH gradient, pH-sensitive Lip have been developed as delivery systems for anticancer agents mainly due to their ability to fuse with the endosomal membrane, triggering the drug release into the cytoplasm (Aghdam et al., 2019; Franco et al., 2021). The responsiveness to pH changes can be obtained if the components of Lip present acid-cleavable bonds or acid-base ionizable groups. Furthermore, tumor tissues usually exhibit hyperthermia due to their rapid metabolism. This phenomenon, besides the higher sensitivity of cancer cells to temperature oscillations, when compared to normal cells (Franco et al., 2021), has prompted the development of thermo-responsive Lip as nanocarriers for delivering anticancer therapeutics (Aghdam et al., 2019; García et al., 2021; Lyon et al., 2018). Lip with responsiveness to temperature changes can be obtained if they incorporate phospholipids with gel-to-liquid crystalline phase transition at a few degrees above physiological temperature (Park et al., 2013), as it has been demonstrated by 1,2-dipalmitoyl-*sn*-glycero-3-phosphocholine (DPPC, Fig. 1**B**), which is a zwitterionic lipid that exhibits a phase transition temperature at around 41 °C (Naitlho et al., 2019).

Moreover, in the development of stimuli-responsive nanocarriers, hybrid nanomaterials composed of both inorganic and organic components have recently been studied. They have demonstrated improved properties combining the ease of processability of the organic component and the mechanical and thermal stability of the inorganic substance (García and Uberman, 2019; Milczewska et al., 2016). One of the strategies that has been explored is the physical or chemical conjugation of

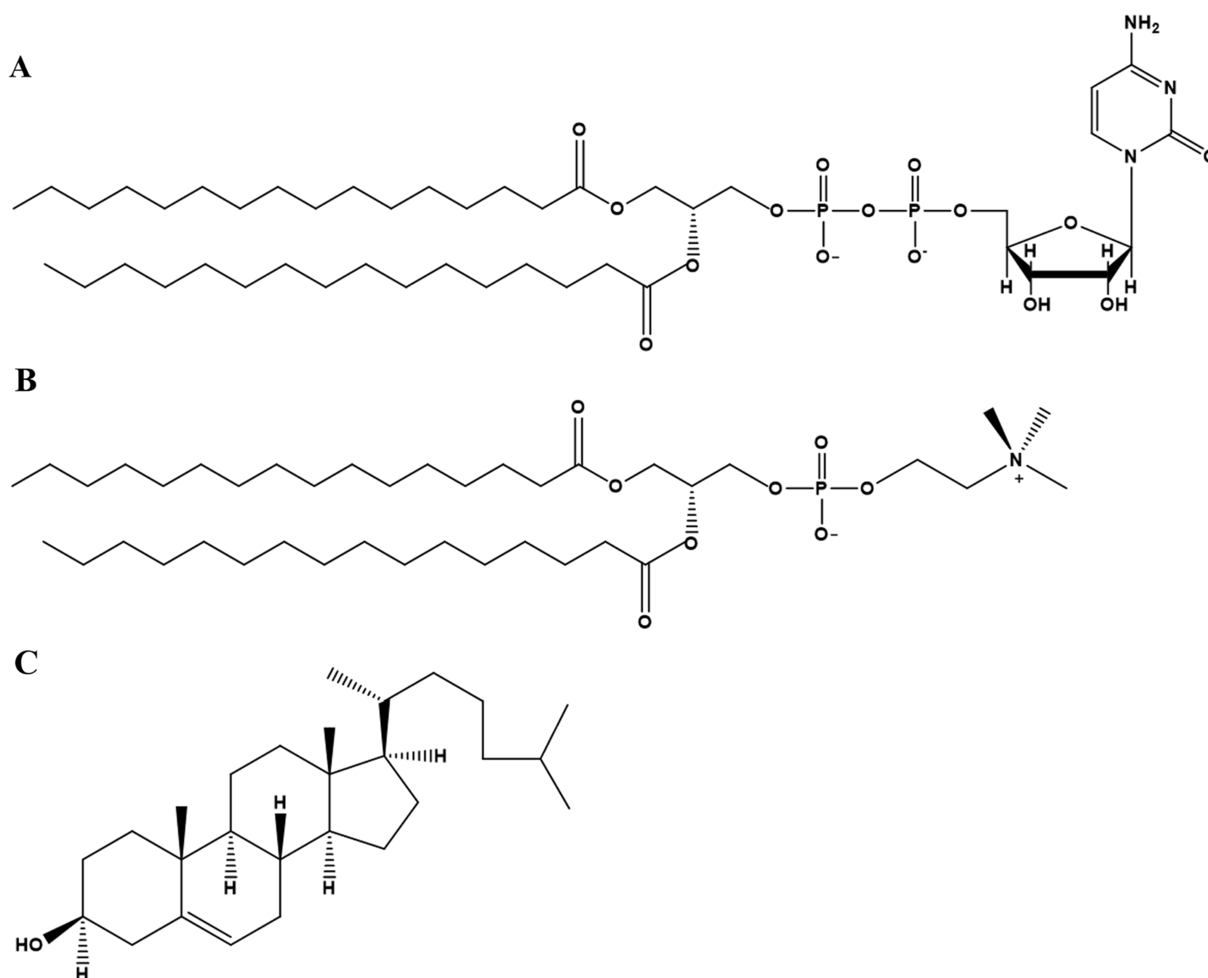

Fig. 1. Molecular structures of **A)** 1,2-dipalmitoyl-*sn*-glycero-3-(cytidine diphosphate) (DG-CDP), **B)** 1,2-dipalmitoyl-*sn*-glycero-3-phosphocholine (DPPC) and **C)** cholesterol.

gold nanoparticles (AuNPs) for anchoring Lip surfaces (Mady et al., 2012), which has proved to be an effective way to increase inorganic nanoparticle stability and biocompatibility under biological conditions (Lozano et al., 2012). AuNPs-functionalized Lip can be used to trigger the drug release in virtue of local temperature changes because of the light-induced heating response of the inorganic component. Thus, these smart hybrid systems can be designed to utilize the photonic properties of AuNPs for local heat generation and trigger content release (Hou et al., 2020; Lajunen et al., 2015; Li and Kataoka, 2020; Sau et al., 2009).

Taking into account these last approaches, in a previous work we developed thermo-sensitive cationic Lip based on DPPC, cholesterol (Fig. 1**C**) and didodecyldimethylammonium bromide (DDAB) at two different ratios (75.24:3.35:21.42 mol% and 45:40:15 mol%), which were then loaded with doxorubicin (Dox) and surface decorated with anionic AuNPs. The influence of cholesterol levels on their interfacial and morphological properties, and drug release profiles were studied. The results obtained showed that the higher the proportion of cholesterol, the higher the drug loading efficiency. Dox was released in a controlled manner and the percentage of drug released was higher as the temperature of the release medium increased, explained by the phase transition of DPPC present into the bilayer. The release was also influenced by the proportion of cholesterol in the liposomal formulations and the drug preserved its anticancer activity when loaded into AuNPs-anchored Lip (García et al., 2021).

The surface functionalization of Lip with AuNPs by complexation requires an appropriate modification of the bilayer composition to confer them surface charge. An alternative with increasing relevance in recent years is the use of Lip that incorporate nucleolipids, which also involves the incorporation of DNA bases into these biomimetic systems (Montis et al., 2012; Rouquette et al., 2019), providing a surface charge to the Lip.

Nucleolipids are amphiphilic compounds formed by the covalent bonding of a nucleoside or nucleotide to the polar head of a lipid chain (Allain et al., 2012). They have aroused great interest in different areas of the biomedical field, such as chemotherapy or gene therapy of cancer (Barthélemy, 2009; Ramzy et al., 2017). Their properties are unique, since they can interact with nucleic acids through specific hydrogen bonds, pi-stacking, or electrostatic forces. The molecular recognition capabilities of these amphiphilic molecules to the complementary DNA base of the base fragment in the nucleolipid molecule have been demonstrated in Langmuir, Langmuir-Blodgett and Langmuir-Shaefer monolayers and bilayers (Alvarez-Malmagro et al., 2019, 2020; Argudo et al., 2019; Michanek et al., 2012; Montanha et al., 2011; Xin et al., 2012). In cancer therapy, the association of these nucleic acid fractions with lipids has been carried out to improve cellular uptake and/or the biodistribution characteristics of nucleosides (Oumzil et al., 2014). Therefore, nucleolipids constitute an excellent model system that combines the self-assembly properties of the phospholipid structure and the specific recognition of the nucleoside fragment, which represents an important advance in the administration and targeting of nucleic acids (Loew et al., 2010; Pokholenko et al., 2013).

With the aim of using nucleolipids like scaffolding material of lipid vesicles for drug loading and delivery, the stability of the lipidic film needs to be optimized. Lateral interactions between adjacent acyl chains play an important role in the stabilization and compact organization of the film. On the other hand, repulsive interactions between polar heads of nucleolipid, either of steric or electrostatic nature, can exert a negative effect on the organization of the molecules in the film. This is particularly relevant in the presence of buffer solution, suggesting that net negative charge of the phosphate groups of the nucleolipid is the main contribution to the repulsive interactions. To address this concern, mixed films of two or three different components can be assembled. In a previous work, the nucleolipid 1,2-dipalmitoyl-*sn*-glycero-3-(cytidine diphosphate) (DG-CDP, Fig. 1**A**) was analyzed in mixed films with DPPC (Prieto-Dapena et al., 2021a) and it was observed that increased the distances between nucleolipid polar heads while identical acyl chains in the whole film were maintained.

The optimum composition of the mixed film can be achieved by thermodynamic analysis of the Langmuir isotherms of the monolayers formed at the air/buffer interface. This can also be performed by including cholesterol in the film formulation, which can be used to provide some extra stabilization of the film.

We hypothesized that a new lipid nanoplatform aimed for triggering delivery of anticancer drugs may be achieved by using a nucleolipid, DP-CDP, as a scaffolding material for preparing lipid vesicles and that its presence in the bilayer constitutes an excellent model system for targeting nucleic acids in cancer therapy, and also that the surface properties conferred by the nucleolipid to the Lip allow the further functionalization with amine-terminated PEGylated-AuNPs.

In this work, we report for the first time DG-CDP-containing lipid vesicles, stabilized by combination with DPPC and cholesterol to design and develop pH-temperature dual-responsive stealth Lip surface functionalized with NH_2-PEGylated-AuNPs for triggering delivery of Dox. Langmuir isotherms of the mixed lipid monolayers were thermodynamically analyzed to define the optimal composition of DG-CDP, DPPC and cholesterol. The drug loading efficiency, interfacial and morphological properties of liposomal formulations were studied as well as the drug release behavior against pH and temperature changes, simulating the conditions in the tumor microenvironment. The anticancer activity of free Dox and loaded into the liposomal formulations was comparatively studied against breast (MDA-MB-231) and ovarian (SK-OV-3) cancer cells.

Dox was selected since it is an anthracycline cytotoxic drug widely used to treat different types of tumors, by a complex mechanism that includes intercalation between the nucleobases of double-stranded DNA, blockage of topoisomerase II, and the generation of free radicals (Sritharan and Sivalingam, 2021; Thorn et al., 2011). Despite its large use as an anticancer agent, this drug causes many side effects, including high cardiotoxicity (Cai et al., 2019; Douedi and Carson, 2019; National Cancer Institute, 2020). Hence, the development of nanostructured systems based in AuNPs-Lip based on the aforementioned components and loaded with this anticancer drug may improve their responsiveness to pH and temperature changes, predicting an effective delivery of Dox to tumors and further reducing its side effects.

2. Materials and methods

2.1. Materials

DPPC and DG-CDP were supplied by Avanti Polar Lipids (Alabaster, AL, USA), and cholesterol and Sephadex® G-50 beads were obtained from Sigma Aldrich® (Barcelona, Spain). NH_2-PEGylated-AuNPs (15 nm) solution was provided by Nanovex Biotechnologies® (Asturias, Spain).

The reagents NaCl, NaOH pellets, Na_3PO_4, KH_2PO_4, K_2HPO_4 and ammonia 30% (PA grade, PanReac AppliChem®, Barcelona, Spain), chloroform stabilized with amylene (EPR grade, LAbKem, Barcelona, Spain), Dox and Triton X-100 solution (Sigma Aldrich®, Barcelona, Spain), HCl 37% (PA grade, T3 Química, Barcelona, Spain), $(NH_4)_2SO_4$ (Sigma Aldrich®, Barcelona, Spain), $CH_3COONa{\cdot}3H_2O$ (AnalaR Normapur, Barcelone, Spain), glacial acetic acid (Labkem, Barcelone, Spain) were used as purchased without further purification. Phosphate buffer solution (PBS) at pH 7.4 (to simulate plasmatic conditions) and acetate buffer solution (ABS) at pH 5.1 (to simulate intracellular endocytic conditions) were prepared according to the United States Pharmacopeia specifications (U.S. Pharmacopoeial Convention, 2015) using analytical grade reagents.

All experiments were carried out with ultra-pure water freshly obtained from a Milli-Q© system.

2.2. Cell cultures

Human breast cancer cells (MDA-MB-231) and human ovarian cancer cells (SK-OV-3) were purchased from the American Type Culture Collection (ATCC) and the Cell Line Service (CLS, Eppelheim, Germany), respectively. Cells were maintained in Dulbecco's Modified Eagle's Medium (DMEM) supplemented with 10% fetal bovine serum, 100 U/mL penicillin and 100 µg/mL streptomycin. All cells were kept in a humidified 37 °C, 5% CO_2 incubator. All cell culture reagents were purchased from Biowest (Nuaillé, France).

2.3. Monolayers of lipids at the air/aqueous interface

Stock solutions of the individual lipid compounds (DPPC, DG-CDP and cholesterol) were prepared in chloroform at concentrations of c.a. 1 mg/mL. The lipid mixtures of different compositions were obtained by adding the required volumes of each lipid stock solution. All lipid solutions were stored at –20 °C. Previously, the glassware used was cleaned in a hot 'piranha' solution (H_2SO_4 98%:H_2O_2 30% in a volume ratio of 3:1) at least 2 h, thoroughly rinsed with ultrapure water and dried overnight in an oven at 80 °C.

Langmuir isotherms were obtained in a PTFE Langmuir trough 611 D from Nima, computer controlled, with a volume of subphase of c.a. 150 cm^3 and maximum interfacial area of c.a. 270 cm^2. Two PTFE moving barriers allowed modification of the interfacial area and surface tension was measured with a PS4 Nima tension sensor using a 1 cm wide chromatographic paper from Whatman®, which was renewed in all measurements. The surface pressure of the monolayer (π) was obtained by the difference between the surface tension in the absence and the presence of the monolayer ($\gamma_0 - \gamma$). The trough was maintained in a Perspex cabinet to avoid contamination from the laboratory atmosphere and interference of airstreams in the pressure sensor.

To obtain the Langmuir isotherm of every monolayer, the trough was cleaned with methanol and water several times. A new Wilhelmy plate was placed hanging from the pressure sensor and the trough was filled with the subphase. The moving barriers were set at the closest position and the interface was aspirated using a new PET pipette tip to eliminate any possible dust from the interface. The barriers were then moved to the open position and the surface pressure sensor lecture was set to zero (γ_0) and a precise volume in the range of 20–30 µL of the lipid solution with the selected composition was spread with a Hamilton chromatographic syringe (0–50 µL) over the subphase and the cabinet was closed. A waiting lapse of 20 min was fixed to allow the solvent evaporation and the monolayer formed was then compressed at a rate of 25 cm^2/min while the surface pressure was measured. All measurements were performed at lab temperature (22 ± 1 °C). The Langmuir isotherms of the

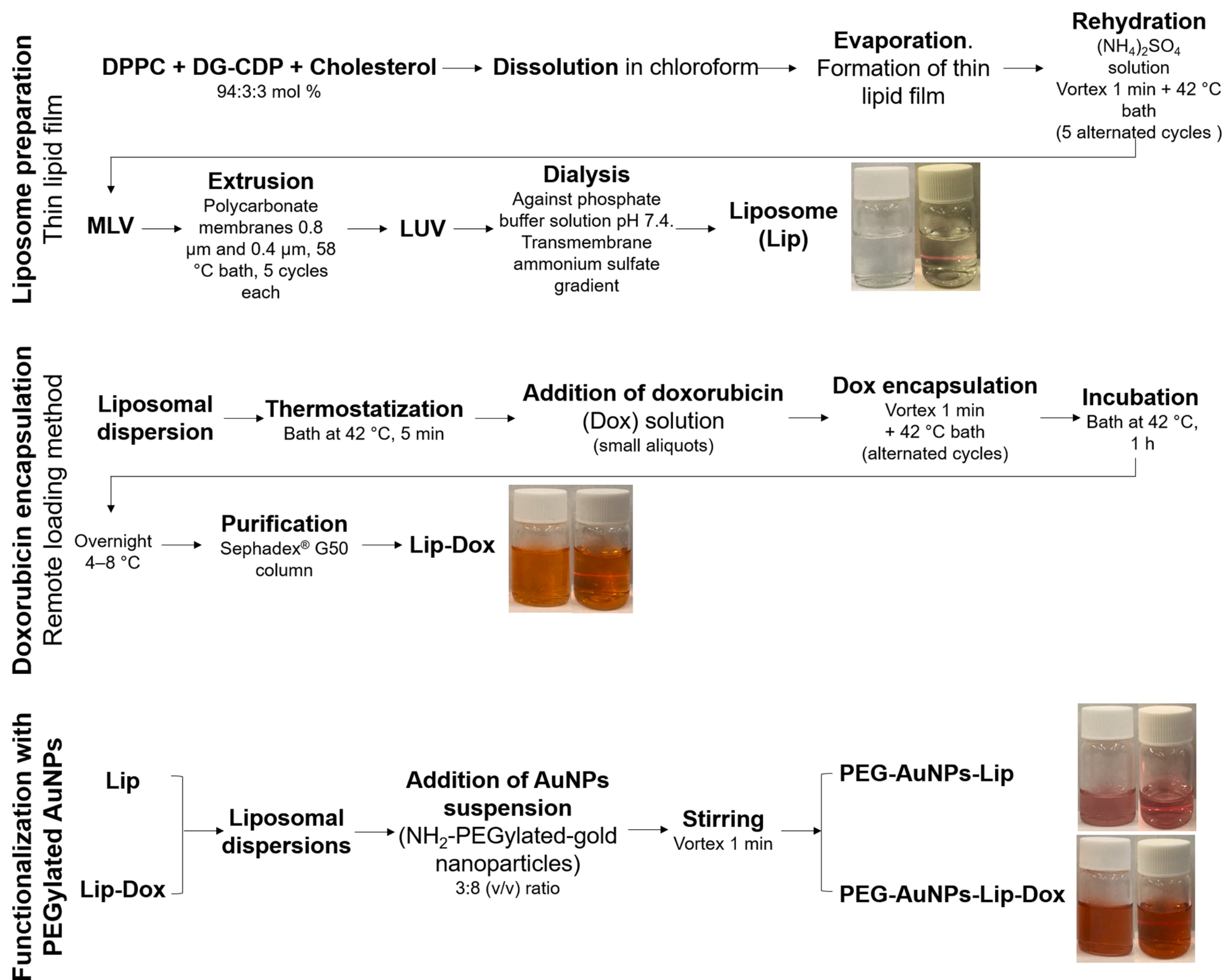

Fig. 2. Schematic representation of the different steps involved in the liposome (Lip) preparation, doxorubicin (Dox) encapsulation and anchoring process with amine-terminated PEGylated gold nanoparticles (NH_2-PEGylated AuNPs). At the end of each step, images of the macroscopic appearance of non-irradiated (left) and laser irradiated (right) liposomal dispersions, showing the Tyndall effect.

monolayers represent the π *vs* the area per molecule (A_{molec}).

2.4. Preparation of unilamellar Lip

The pre-weighed components (DPPC, DG-CDP and cholesterol) at a ratio of 94:3:3 mol% were dissolved in chloroform. The sample was evaporated (Büchi®, R-200) at 42 °C, the organic solvent was removed and a thin lipid film was obtained, which was then hydrated by adding 3 mL of 250 mM $(NH_4)_2SO_4$ aqueous solution. Multilamellar Lip were formed after 5 alternated cycles consisting of stirring by vortex for 1 min and heating bath at 42 °C for 5 min.

The liposomal formulations were then processed as previously described (García et al., 2021), with some modifications. Briefly, 2 mL of sample were placed in an extruder (Avanti Polar Lipids®, Alabaster, AL, USA) under airflow and a heating bath at 58 °C, and extruded through 0.8 μm polycarbonate membranes followed by 0.4 μm polycarbonate membranes, 5 times each to obtain unilamellar Lip. The liposomal formulations were then dialyzed to generate a transmembrane ammonium sulfate gradient between lipid vesicle core and external media/continuous phase. The dispersion of unilamellar Lip was taken inside a cellulose dialysis bag (10 kDa) and dialyzed against PBS pH 7.4 in a volume ratio of 1:600 for 6 h, at room temperature (23–25 °C), and under magnetic stirring.

Fig. 2 shows a schematic representation of liposome preparation.

2.5. Dox loading and purification

Remote loading method was used to encapsulate Dox into Lip, as previously described (García et al., 2021), with some modifications. Shortly, liposomal dispersions were incubated in a heating bath (42 °C, 5 min). Small aliquots of Dox aqueous solution at a concentration of 1 mg/mL were added to Lip, alternating with cycles of stirring by vortex for 1 min and heating bath at 42 °C. After adding the pre-determined amount of Dox, the Lip-Dox dispersions were incubated for 1 h at 42 °C and then left overnight at 4–8 °C.

Purification process was applied to remove the unloaded Dox. Sephadex® G-50 beads were hydrated in previously degassed PBS pH 7.4. Syringes of 2 mL without needles were used to prepare the purification columns, following the same procedure described in a previous work (García et al., 2021) while PBS 7.4 was used as elution fluid. The eluted Lip-Dox colloidal dispersions were followed by direct observation under laser-induced effect of light scattering (Tyndall effect). The Dox-loaded Lip were eluted in the first 1.5 mL and collected for further studies. Free Dox was also collected, which eluted after adding 3 mL of PBS pH 7.4.

Fig. 2 shows a schematic representation of Dox encapsulation in liposomal nanocarriers.

2.6. Anchoring with NH_2-PEGylated-AuNPs

Unloaded and Dox-loaded Lip were surface functionalized with PEG-AuNPs by complexation after adding a suspension of NH_2-PEGylated-AuNPs to the liposomal dispersions in a 3:8 (*v/v*) ratio and stirred with a vortex for 1 min.

Fig. 2 shows a schematic representation of the anchoring process with NH_2-PEGylated AuNPs once the Lip and Dox-loaded Lip were obtained.

2.7. Characterization of liposomal dispersions

2.7.1. Size and surface charge

The apparent hydrodynamic diameter (d_H) and zeta potential (ζ) were determined by measurements of dynamic light scattering and electrophoretic light scattering, respectively, using a Zetasizer Nano-S instrument (Malvern Instruments®, Malvern, UK). The cumulant method and the CONTIN algorithm were used to calculate the d_H values and size distributions, respectively. Polydispersity indexes (PDI) were also determined. The Smoluchowski equation was used to convert electrophoretic mobilities to ζ. All measurements were made in triplicate at room temperature (23–25 °C).

2.7.2. Field-emission scanning electron microscopy (FE-SEM)

The morphological analysis of liposomal dispersions was carried out in an FE-SEM microscope (Hitachi® S5200, Hitachi, Krefeld, Germany). For sample preparation, 40 μL of each dispersion were placed in a Si sample holder and observed (uncovered samples). Samples coated with sputtered Pt in Ar atmosphere in a high vacuum evaporator were also analyzed (covered samples). The images were then obtained at an excitation voltage of 5 kV.

2.7.3. Encapsulation efficiency

The amount of encapsulated Dox in the liposomal dispersions was determined by absorbance measurements at 480 nm (Agilent® 8453 System, Agilent, Victoria, Australia) after lysis of Lip with Triton X-100 (final concentration 0.5% *v/v*). The percentage of encapsulation efficiency (EE %) was determined according to Equation (1):

$$EE\ \% = \frac{Dox_E}{Dox_T} \times 100 \quad (1)$$

where Dox_T is the total amount of drug added to prepare the Dox-containing Lip and Dox_E is the amount of Dox quantified after lysis of Lip, thus corresponding to the encapsulated drug. To confirm these results, the EE % was also indirectly determined by quantifying Dox solution samples eluted in the purification process (see Section 2.5).

2.8. In vitro drug release studies

Dox-loaded liposomal dispersions were subjected to drug release analysis. The release rate from an aqueous solution with an equivalent concentration of Dox was used as a reference. Experiments were performed in Franz diffusion cells mounted with a semisynthetic cellulose membrane (molecular cut-off 10 kDa), which was placed between the donor and the receptor compartments. 1 mL of each sample was carefully placed in the donor compartment and kept in contact with 14.5 mL of receptor medium (PBS pH 7.4 and ABS pH 5.1). Samples of 1 mL of receptor medium were withdrawn at predetermined time intervals and replaced with equivalent volumes of preheated fresh medium. The concentration of Dox in the samples was determined by UV–Vis spectrophotometry at 480 nm (Agilent® 8453 System, Agilent, Victoria, Australia), using calibration curves constructed for each receptor medium. All experiments were carried out in triplicate and the sink conditions were maintained. The cumulative percentage of Dox released was calculated and expressed as a function of time. The results were expressed as the % average of three determinations with their respective SD.

The Dox release profiles from the liposomal dispersions and the reference sample were statistically compared using the difference factor (f_1) and the similarity factor (f_2) (Equations (2) and (3), respectively). According to this methodology, a f_1 value above 15 and a f_2 value in the 0–49 range implies a difference between the release profiles (Costa and Lobo, 2001).

$$f_1 = \frac{\sum_{t=1}^{n} |R_t - T_t|}{\sum R_t} \times 100 \quad (2)$$

$$f_2 = 50 \times log\left\{ \left(1 + \left(\frac{1}{n}\right) \sum_{t=1}^{n} (R_t - T_t)^2 \right)^{-0.5} \times 100 \right\} \quad (3)$$

where n is the number of sampling time points, $\sum$ is the summation over all time points and R_t and T_t are the cumulative percentages of drug released at each of the n time points of the reference and test sample,

respectively. The CV was below 15% in all cases. Only one point after 85% of drug release was used for each equation.

The mean release profiles at each release medium were fitted according to common mathematical models, corresponding to Zero order, Higuchi and Korsmeyer–Peppas (Equations (4), (5) and (6), respectively) (Costa and Lobo, 2001; Jain and Jain, 2016).

$$\frac{Dox_t}{Dox_0} = k_Z \times t \tag{4}$$

$$\frac{Dox_t}{Dox_0} = k_H \times t^{0.5} \tag{5}$$

$$\frac{Dox_t}{Dox_0} = k_P \times t^n \tag{6}$$

where Dox_t (%) is the percentage of drug released at time t; Dox_0 is the initial value of Dox_t, t is the time; n is the diffusion release exponent; and k_Z, k_H, and k_P are the kinetic constants corresponding to Zero order, Higuchi and Korsmeyer–Peppas kinetic models, respectively.

2.9. *In vitro anticancer activity*

The anticancer activity of Dox-loaded liposomal formulations (Lip-Dox and PEG-AuNPs-Lip-Dox) was studied against MDA-MB-231 and SK-OV-3 cancer cells and compared with the cytotoxicity exhibited by free Dox. Cell viability was evaluated by a colorimetric assay, resazurin. This assay is based on the reduction of the blue compound resazurin by viable cells into the pink-soluble product resorufin. The quantity of resorufin produced is proportional to the number of viable cells. Briefly, exponentially growing cells were seeded in 96-well plates and allowed to grow for 24 h. Cells were then exposed to the treatments for 2 h and allowed to grow for an additional 70 h in drug-free medium; or cells were continuously treated for 72 h. After incubation times, cells were washed once with PBS pH 7.4, and 150 μL resazurin (20 μg/mL in medium) were added to each well. The plates were incubated for 5 h at 37 °C and 5% CO_2, and, then the optical densities were measured at 540 nm and 620 nm with an absorbance spectrophotometer microplate reader (Multiskan EX Labsystems). Cell viability was expressed as a percentage respect to the untreated cells (control). Results were expressed as mean ± SEM. All data are from two independent experiments.

3. Results

3.1. *Langmuir isotherms and thermodynamic analysis*

Langmuir isotherms of mixed DPPC/DG-CDP monolayers were measured at the air/NaF 0.1 M interface of the Langmuir trough, at different mole fractions of the nucleolipid (x_{DG-CDP}). Fig. 3**A** shows a representative sample of the registered isotherms. It can be observed that the increase in the mole fraction of the nucleolipid also increased

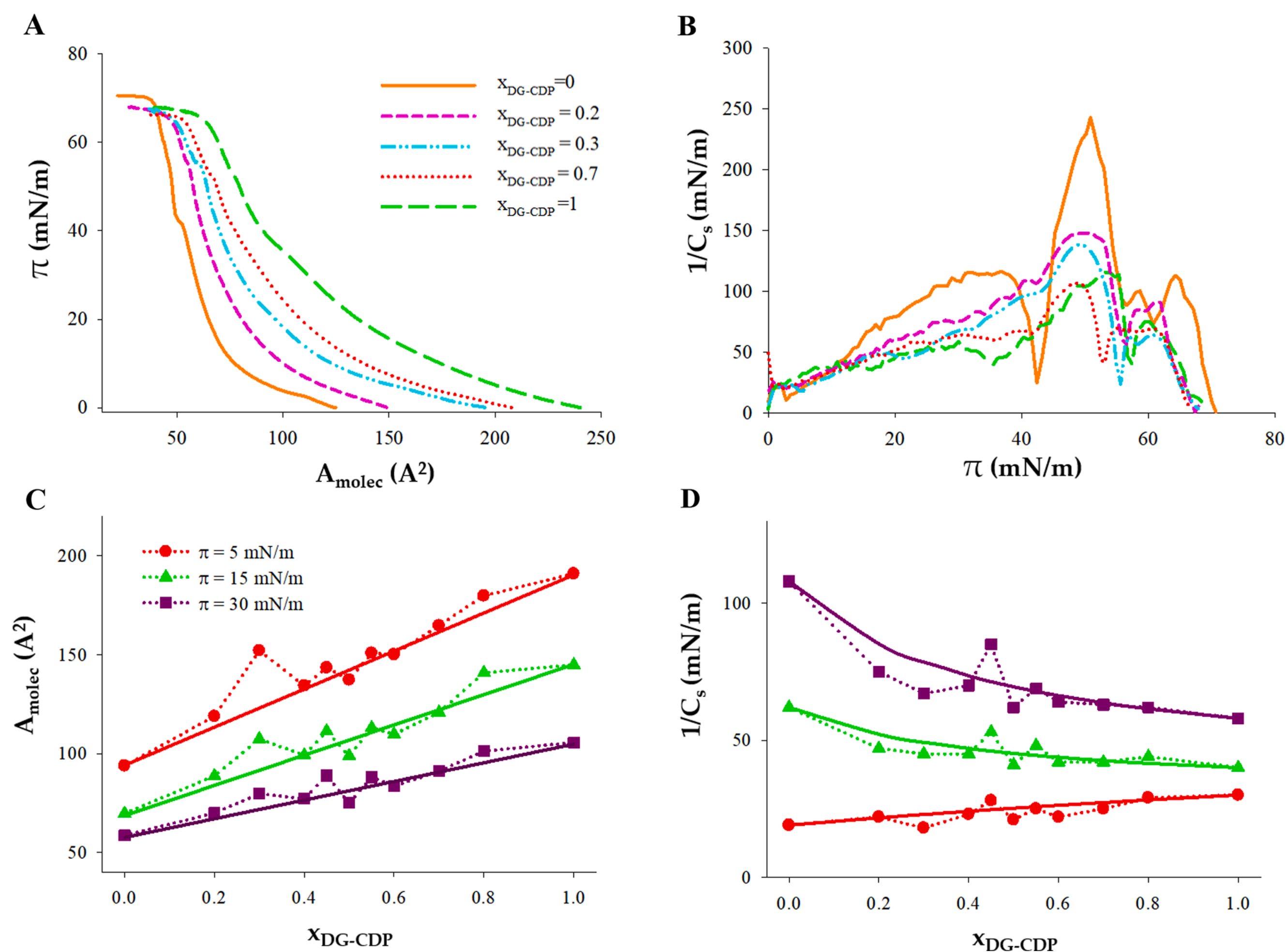

Fig. 3. A) Langmuir isotherms in the air/NaF 0.1 M interface for mixed DPPC/DG-CDP monolayers with the mole fraction of the nuclelipid DG-CDP (x_{DG-CDP}) indicated in the figure. **B)** Compressibility elastic modulus ($1/C_s$) of the monolayers in **A** plotted as a function of surface pressure (π). **C)** Area per molecule (A_{molec}) and **D)** $1/C_s$ *vs.* mole fraction of nucleolipid (x_{DG-CDP}) at the surface pressure values indicated in figure **C**. Solid lines in **C** and **D** represent the ideal plots calculated with Equations (8) and (9).

the averaged A_{molec} of the mixed films at constant π. In addition, the isotherms adopted a lower slope in the entire surface pressure range. It evidenced a higher fluidity of the films, that could be quantified with the elastic compressibility modulus ($1/C_s$), defined as described in Equation (7).

$$\frac{1}{C_s} = -A_{molec}\frac{d\pi}{dA_{molec}} \tag{7}$$

Compressibility modules *vs*. the surface pressure (π) are plotted in Fig. 3**B**. It can be observed that only the pure DPPC monolayer reached $1/C_s$ values higher than 200 mN/m, characteristic of a solid-like behavior. At the approximate equilibrium pressure of the DPPC monolayers, 30 mN/m, they behaved almost like a liquid condensed phase, with a $1/C_s > 100$ mN/m. In contrast, the monolayers containing DG-CDP exhibited values of the $1/C_s$ that were characteristics of a liquid expanded phase. This effect was more evident as the nucleolipid concentration increased.

Deviations from the ideality of the lipid's mixture could be detected by plotting the A_{molec} and the $1/C_s$ *vs* the x_{DG-CDP} at constant pressure, as can be observed in Fig. 3**C and 3D.**

In an ideal mixture, the A_{molec} and $1/C_s$ values must be averaged considering that DPPC and DG-CDP molecules did not change these values when they were in a pure component monolayer or a mixed monolayer. Then, A_{molec}^{ideal} and C_s^{ideal} can be calculated according to Equations (8) and (9).

$$A_{molec}^{ideal} = x_{DG-CDP}\cdot A_{molec(x_{DG-CDP}=1)} + (1 - x_{DG-CDP})\cdot A_{molec(x_{DG-CDP}=0)} \tag{8}$$

$$C_s^{ideal} = -\frac{1}{A_{molec}^{ideal}}\left[x_{DG-CDP}\cdot A_{molec(x_{DG-CDP}=1)}\cdot C_{s(x_{DG-CDP}=1)} + (1 - x_{DG-CDP})\cdot A_{molec(x_{DG-CDP}=0)}\cdot C_{s(x_{DG-CDP}=0)}\right] \tag{9}$$

The ideal values of A_{molec} and $1/C_s$, included in Fig. 3**C and 3D,** were almost coincident with the experimental values, suggesting an ideal behavior of the two components in the mixture.

In order to decrease the fluidity of the nucleolipid-containing lipidic film, variable ratios of cholesterol were added to the mixture with a 7:3 DPPC:DG-CDP mole ratio. The corresponding π *vs*. mean A_{molec} were registered and the compression elastic moduli were calculated (Fig. 4**A and 4B**). The results clearly showed that to obtain a gel-like behavior, at a surface pressure of 30 mN/m, it would be necessary a mole fraction of cholesterol higher than 0.6, which is too high.

3.2. Morphological and interfacial properties and drug loading efficiency

Fig. 2 shows the macroscopic appearance of liposomal dispersions under non-irradiation (left images) and laser irradiation (right images), showing the Tyndall effect of them because of their colloidal properties. Table 1 summarizes the results of d_H, PDI, ζ and EE % of the different liposomal dispersions as well as the NH_2-PEGylated-AuNPs suspension. As observed, all liposomal formulations exhibited sizes on the nanometer scale, with a size range of approximately 400 to 650 nm. The size increased as increased the complexity of the lipid system. PEG-AuNPs-functionalized Lip unloaded and loaded with Dox exhibited higher d_H than their respective counterparts without the PEG-AuNPs anchoring. The NH_2-PEGylated-AuNPs showed a small size, according to the information provided by the manufacturer. PDI values were acceptable in all the analyzed samples (PDI ≤ 0.35). The presence of the nucleolipid provided to the Lip serie a negative surface charge. Anchoring with positively charged NH_2-PEGylated-AuNPs induced an increase in the ζ values of both unloaded and Dox-loaded Lip, which was greater for the

Table 1
Hydrodynamic apparent diameter (d_H), polydispersity index (PDI), zeta potential (ζ) and encapsulation efficiency (EE %) of unloaded and doxorubicin (Dox)-loaded nucleolipid-containing liposomes (Lip and Lip-Dox, respectively) with and without functionalization with NH_2-PEGylated gold nanoparticles (PEG-AuNPs-Lip and PEG-AuNPs-Lip-Dox, respectively). The properties of pure PEG-AuNPs are also described.

Sample	d_H (nm)	PDI	ζ (mV)	EE %
Lip	415 ± 7	0.19 ± 0.01	–23 ± 1	–
PEG-AuNPs	17 ± 1	0.25 ± 0.01	+69 ± 3	–
PEG-AuNPs-Lip	479 ± 9	0.27 ± 0.04	–18.2 ± 0.2	–
Lip-Dox	535 ± 9	0.30 ± 0.03	–14.7 ± 0.1	82 ± 5
PEG-AuNPs-Lip-Dox	651 ± 9	0.33 ± 0.01	–6.6 ± 0.3	78 ± 4

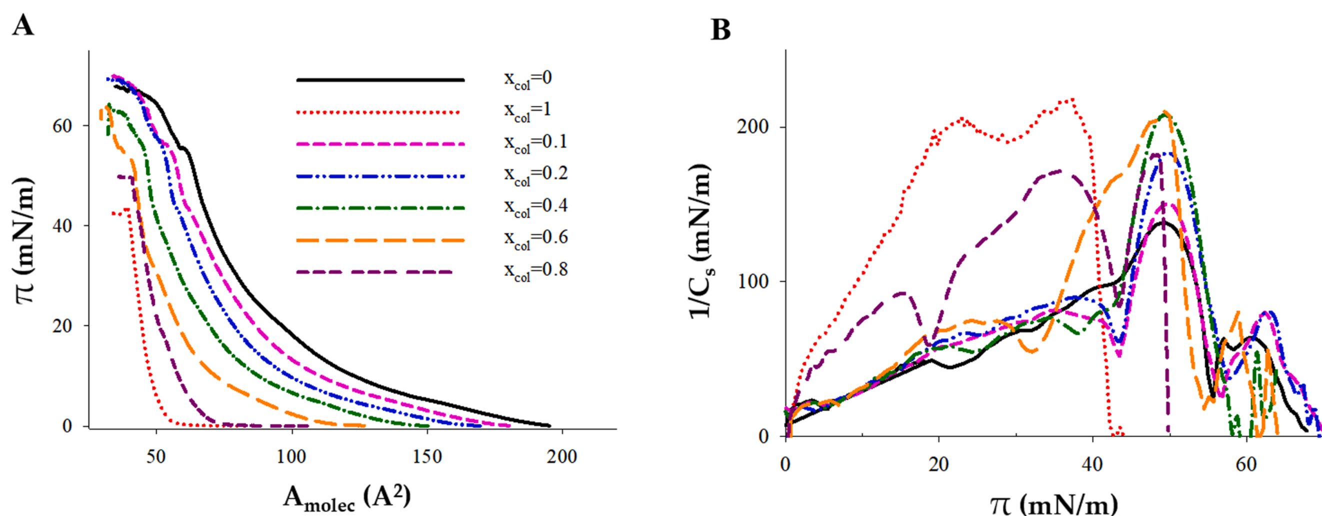

Fig. 4. A) Langmuir isotherms in the air/NaF 0.1 M interface for mixed DPPC/DG-CDP monolayers with the mole fraction of cholesterol (x_{chol}) indicated in the figure. **B)** Compressibility elastic modulus ($1/C_s$) of the monolayers in **A** plotted as a function of surface pressure (π).

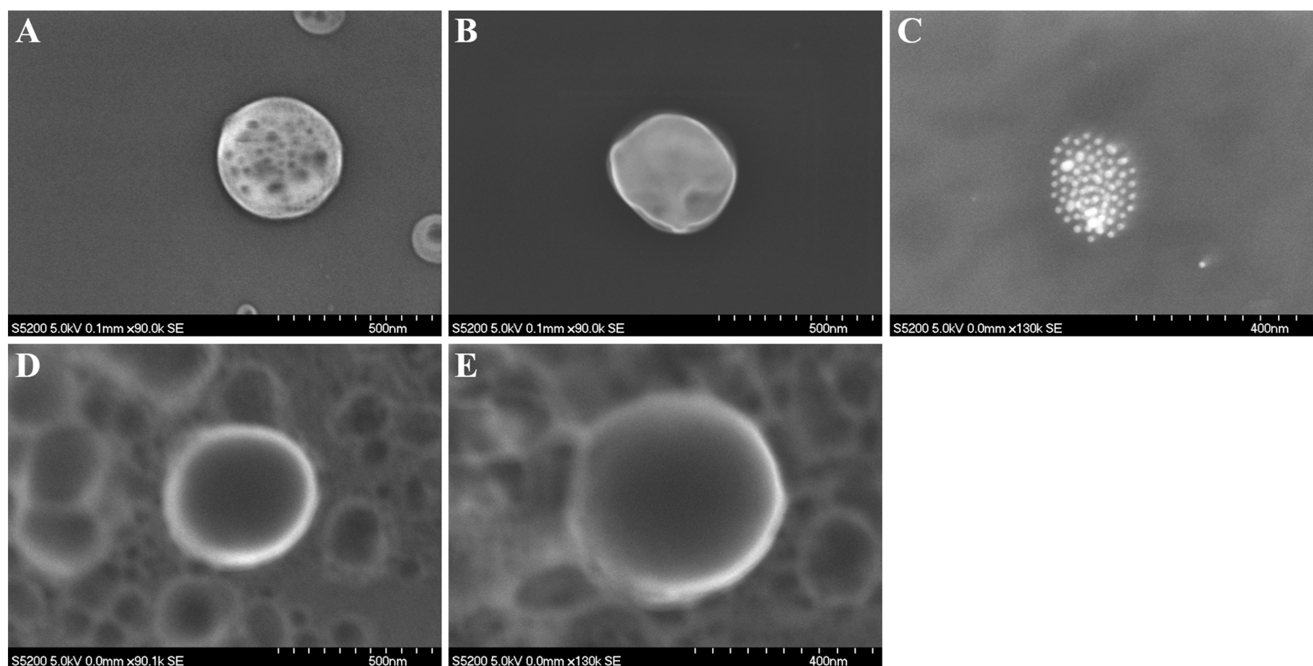

Fig. 5. FE-SEM images of (**A**) Lip, (**B**) Lip-Dox, (**C**) PEG-AuNPs, (**D**) PEG-AuNPs-Lip, and (**E**) PEG-AuNPs-Lip-Dox. **A, B** and **D**, scale bar: 500 nm, **C** and **D**, scale bar: 400 nm. Lip: nucleolipid-containing liposomes; Dox: doxorubicin, and PEG-AuNPs: NH_2-PEGylated gold nanoparticles.

latter. Lip-Dox displayed a slightly higher mean EE % value compared to the PEG-AuNPs-Lip-Dox.

The morphology of liposomal formulations and NH_2-PEGylated-AuNPs, as well as PEG-AuNPs decorated Lip, was analyzed by FE-SEM (Fig. 5). Unloaded and Dox-loaded Lip with and without functionalization with PEG-AuNPs displayed approximately spherical shapes on the nanometer scale with sizes comparable to those obtained by dynamic light scattering. NH_2-PEGylated-AuNPs also exhibited a spherical shape, small sizes and discrete nanoparticles were observed in the sample with almost depreciable agglomeration. The PEG-AuNPs

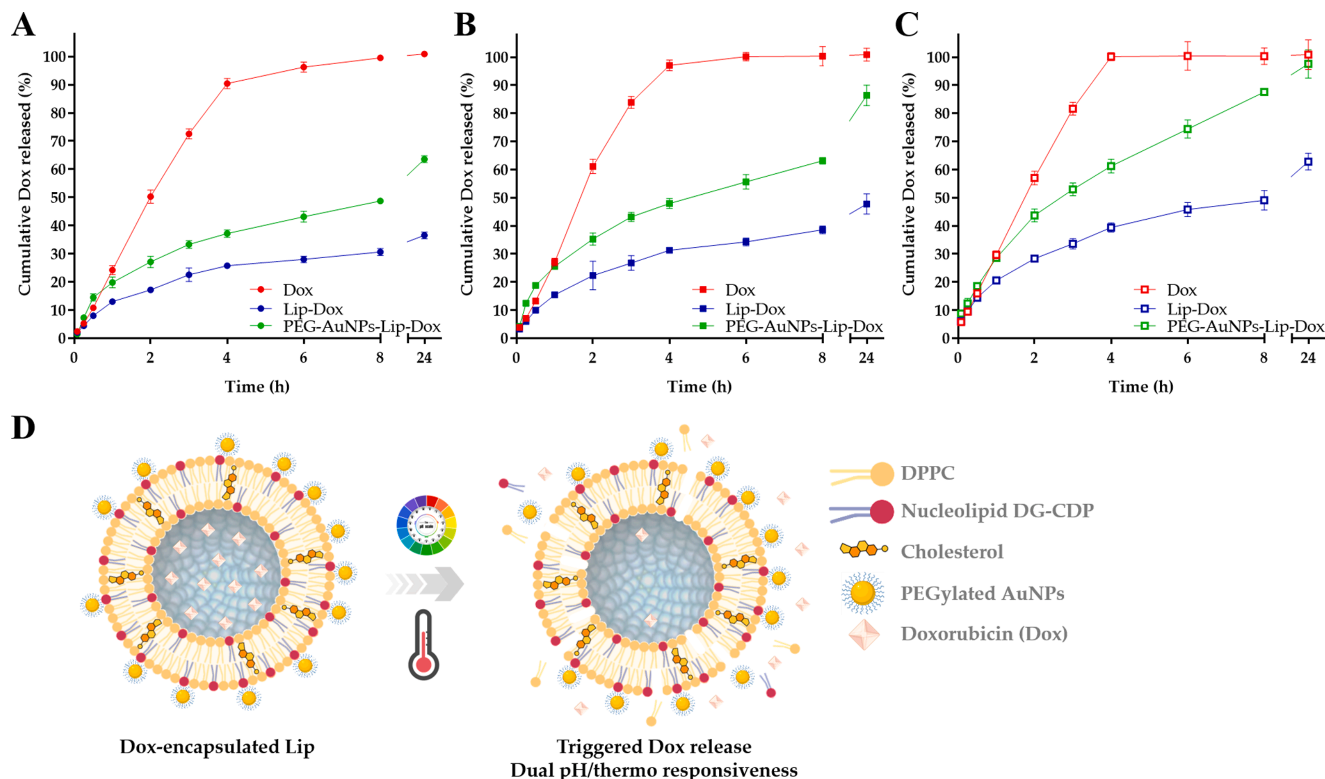

Fig. 6. Effects of pH and temperature on the *in vitro* release of doxorubicin (Dox) from liposomal formulations. Release profiles obtained in (**A**) PBS pH 7.4 at 37 °C, (**B**) ABS pH 5.1 at 37 °C and (**C**) ABS pH 5.1 at 42 °C. *In vitro* Dox release profiles from the free drug are also displayed. **D)** Schematic depiction of the Dox-loaded nucleolipid-based Lip anchored with PEGylated AuNPs and their dual responsiveness to pH and temperature changes for triggering delivery of Dox. Lip-Dox: nucleolipid-containing Dox-loaded liposomes and PEG-AuNPs-Lip-Dox: NH_2-PEGylated gold nanoparticles anchored on the surface of Lip-Dox.

decorating the surfaces of both Lip, with and without Dox, was visualized in the corresponding samples, which showed a greater white brightness on their outside. In Lip sample, some porous were observed while they disappeared in all the other liposomal samples.

3.3. In vitro release of Dox

The *in vitro* release profiles of Dox from liposomal formulations toward PBS pH 7.4 and ABS pH 5.1, simulating physiological and lysosomal conditions, respectively, at 37 °C and 42 °C as receptor media were analyzed. Fig. 6 shows cumulative Dox release percentages as a function of the time. The release profiles of a reference sample of pure Dox are also depicted.

Dox was released in a controlled manner towards both media (acidic- and neutral-pH environment) at the two temperatures evaluated (physiological and hyperthermia values), being more sustained from Lip-Dox than from PEG-AuNPs-Lip-Dox; while the release of Dox reference sample was faster, reaching almost 100% of drug released at 6 h and 4 h toward PBS pH 7.4 and ABS pH 5.1, respectively.

Negligible *burst* effects were observed for the different samples toward physiological conditions. Slight *burst* effects were observed for Lip-Dox toward acidic medium in the first 15 min, reaching up to 6% and 9.5% at 37 °C and 42 °C, respectively. Important *burst* effects were observed from PEG-AuNPs-Lip-Dox at pH 5.1 at both temperatures, reaching approximately 13% of Dox released in the first 15 min.

A lower leakage of the drug release was achieved from both liposomal formulations toward physiological pH and temperature compared to the Dox release in an acidic environment, which increased even at higher temperature. As observed, at any time, the PEG-AuNPs-Lip-Dox formulation released major percentages of Dox at pH 5.1 compared to pH 7.4, reaching approximately 63% and 50%, respectively (32.6 and 47.9 for f_1 and f_2 values, respectively), and the drug release was even augmented at 42 °C in comparison to 37 °C (64.2 and 45.9 f_1 and f_2 values, respectively), reaching almost 88% of drug release at 8 h of the assay. This triggered effect produced at acidic pH and hyperthermia temperature indicated the responsiveness to both stimuli from the nucleolipid-containing stealth Lip. Non-significant differences were observed in the release profiles of Dox from Lip-Dox formulations towards pH 7.4 and 5.1 at 37 °C ($f_1 = 14.2$ and $f_2 = 53.4$), from which the percentages of drug release reached almost 30% and 38%, respectively. However, a significant increase in the percentage of drug release was observed at 42 °C compared to 37 °C ($f_1 = 31.3$ and $f_2 = 47.9$), reaching approximately 50% of Dox release at 8 h of the experiments.

Kinetic analysis of *in vitro* release data using Zero order, Higuchi and Korsmeyer-Peppas equations were carried out to evaluate the main mechanism of Dox transport through the lipid-based nanostructures. Results of kinetic data are summarized in Table 2. At pH 5.1, release data plotted as Higuchi and Korsmeyer-Peppas models were found to be fairly linear for both liposomal formulations, Lip-Dox and PEG-AuNPs-Lip-Dox, which was also supported by their regression coefficient values ($R^2 > 0.985$ and $R^2 > 0.994$, respectively). Furthermore, n values in the range of 0.481–0.592 confirmed that the kinetics of Dox release from these formulations indicated a Fickian transport with a preponderant release mechanism controlled by drug diffusion. These results were in good correlation with the R^2 values obtained by applying the Higuchi model. In particular, in the case of PEG-AuNPs-Lip-Dox, the $n > 0.5$ suggested that even the main mechanism of drug release is diffusion-controlled, other mechanisms such as membrane permeability, disruption, etc. could also occur. At pH 7.4, release data of Lip-Dox fitted to Korsmeyer-Peppas model ($R^2 > 0.978$) with a n value near 0.5, indicating a Fickian transport. Under this release condition, the Dox release profile from PEG-AuNPs-Lip-Dox (plotted as the Higuchi model) was found to be fairly linear ($R^2 > 0.995$), suggesting a main release mechanism controlled by drug diffusion. In the case of the Dox reference sample, independent of the pH and temperature of the release media the release profiles were well fitted to Zero order ($R^2 > 0.996$), indicating a constant release rate.

3.4. In vitro anticancer activity

The Resazurin assay was used to evaluate whether Dox-loaded liposomal formulations could preserve its cytotoxicity against cancer cells. Because Dox, alone or in combination with other drugs, has been widely used as the first-line to treat a variety of metastatic tumors, including breast and ovarian cancer, we chose the human breast carcinoma cell line MDA-MB-231 and the human ovarian adenocarcinoma cell line SK-OV-3 as *in vitro* models. To study the influence of the release kinetic characteristics of Dox from Lip and AuNPs-Lip on its cytotoxicity, cells were exposed for 2 h to the treatments, followed by an additional period of 70 h in drug-free medium; or cells were continuously treated for 72 h.

Results of resazurin assay (Fig. 7) clearly showed that the cytotoxic activity of Dox loaded into non-functionalized and AuNPs-functionalized Lip was time-dependent. Fig. 7**A and 7B** show that the antiproliferative effect of free Dox was higher than that of Dox released from liposomal dispersions after 2 h of treatment. Cell viability for both cell lines was approximately 60% after 2 h of exposure to the highest concentration tested of free Dox, while Dox-loaded Lip and AuNPs-Lip were found to be slightly cytotoxic (cell viabilities > 80%). These results are consistent with the data shown in Fig. 6 since liposomal dispersions released approximately 15–25% Dox during the first two hours at pH 7.4 and 37 °C, the same as the cell culture conditions used. Therefore, these data show that Dox was not immediately released from Lip. Dox-unloaded Lip did not have a remarkable cytotoxic effect against both cell lines (data not shown).

Fig. 7**C and 7D** showed that the developed formulations (Lip-Dox

Table 2
Kinetic data obtained from doxorubicin (Dox) release studies toward PBS pH 7.4 and ABS pH 5.1 at two different temperatures, using Zero order, Higuchi and Korsmeyer-Peppas equations.

Temperature	Release medium	Kinetic Models							
		Sample	Zero Order		Higuchi		Korsmeyer-Peppas		
			k_Z	R^2	k_H	R^2	k_P	n	R^2
37 °C	PBS pH 7.4	Dox	24.9	0.999	50.1	0.978	23.3	1.068	0.998
		Lip-Dox	4.9	0.976	10.7	0.965	13.3	0.425	0.978
		PEG-AuNPs-Lip-Dox	4.9	0.909	16.2	0.995	18.2	0.531	0.971
	ABS pH 5.1	Dox	26.0	0.999	58.3	0.983	27.0	0.974	0.999
		Lip-Dox	5.9	0.974	14.0	0.998	15.1	0.483	0.985
		PEG-AuNPs-Lip-Dox	6.2	0.925	21.6	0.994	25.2	0.481	0.997
42 °C	ABS pH 5.1	Dox	26.3	0.996	53.5	0.964	31.6	0.759	0.980
		Lip-Dox	8.2	0.955	18.8	0.997	19.8	0.489	0.997
		PEG-AuNPs-Lip-Dox	0.9	0.950	31.6	0.998	28.3	0.592	0.999

k_Z, k_H and k_P expressed as % h^{-1}, % $h^{-0.5}$ and % k^{-n}, respectively. Experimental data correspond to 5–60% of Dox released. Lip-Dox: nucleolipid-containing Dox-loaded liposomes and PEG-AuNPs-Lip-Dox: NH_2-PEGylated gold nanoparticles anchored on the surface of Lip-Dox.

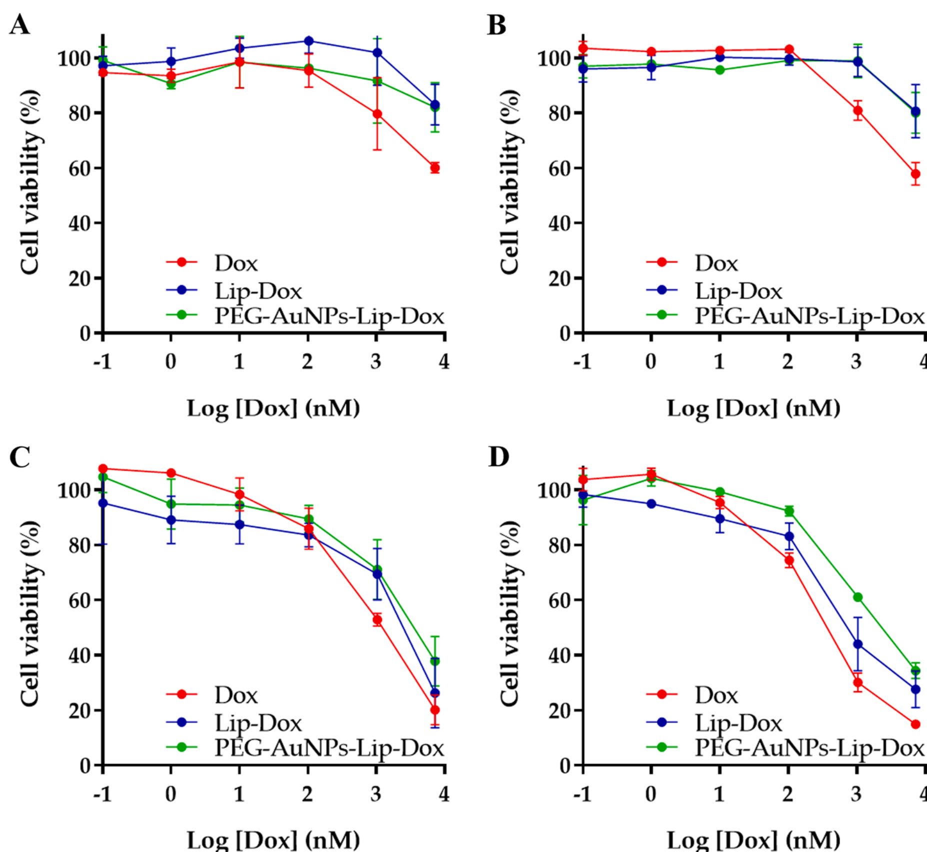

Fig. 7. Cytotoxicity of free doxorubicin (Dox) and Dox-loaded liposomes (Lip-Dox and PEG-AuNPs-Lip-Dox) against MDA-MB-231 breast cancer cells (A and C) and SK-OV-3 ovarian cancer cells (B and D). Cells were exposed to the treatments for 2 h and allowed to grow for an additional 70 h in drug-free medium (A-B); or cells were continuously treated for 72 h (C-D). Finally, cell viability was measured with the resazurin assay. The concentrations of the Lip represented in the graphs are those used to deliver the concentrations of Dox shown on the x axis of the graphs (log10 concentration of Dox). Data are reported as means ± standard error of mean (SEM) and were obtained from two independent experiments.

and PEG-AuNPs-Lip-Dox) showed high cytotoxicity in both cell lines, suggesting that Dox was released from these formulations over time. The inhibitory concentration 50 (IC_{50}) values (mean ± SEM, nM) of free Dox, Lip-Dox and PEG-AuNPs-Lip-Dox in MDA-MB-231 cells were 1403.0 ± 336.2, 3294.8 ± 911.9 and 3562.7 ± 1502.5, and in SK-OV-3 were 373.8 ± 60.2, 978.5 ± 523.3 and 2350.9 ± 288.5, respectively. Both Dox-loaded Lip and AuNPs-Lip displayed less cytotoxicity than free Dox, probably as a consequence of slower Dox release kinetic characteristics under cell culture conditions (pH 7.4 and 37 °C). Cell lines are adapted to grow under specific conditions, which limits the possibilities of changing temperature and pH.

4. Discussion

Cancer nanomedicine is a promising approach to overcome limitations of current anticancer treatments. Nano-scale systems provide numerous advantages, including enhanced drug delivery to tumor tissue and, therefore, minimizing the side effects in the rest of the organism. Although several Dox-containing liposomal formulations have already been developed to reduce Dox-induced cardiotoxicity (Beltrán-Gracia et al., 2019), they have shown limitations and pharmacological problems, such as low half-life due to rapid clearance by the host's immune system. Therefore, novel formulations are needed to overcome their limitations, among which those designed to release their cargo only when exposed to a specific trigger stimulus at the tumor site, preventing or minimizing drug release in the bloodstream and normal tissues (Aghdam et al., 2019), as well as those with stealth surfaces (Franco et al., 2021) that allow optimal anticancer effects to be achieved and prevent the immune system with the subsequent clearance from the systemic circulation. Here we report for the first time the design, development and evaluation of DG-CDP-containing pH-temperature dual-responsive Lip to trigger the delivery of anticancer drugs such as Dox.

When lipid-based formulations are prepared with mixtures of the lipid components, their proportion is critical because it determines the stability of the obtained Lip. Fig. 3**A** shows that the A_{molec} increased at constant π with the mole fraction of DG-CDP. Taking into account that the acyl chains of DPPC and DG-CDP are identical, the increase in the A_{molec} must be caused by repulsive interactions, either electrostatic and steric, between the nucleolipid polar heads. In a previous paper (Prieto-Dapena et al., 2021a), the charge number per DG-CPD molecule in mixed DPPC/nucleolipid monolayers transferred to gold electrodes was determined to be between −1.5 and −2 units, explaining repulsive interactions between the polar heads of close DG-CPD molecules. Moreover, the cytosine moiety of DG-CDP was demonstrated to be tilted towards the monolayer, probably as a consequence of H-bonding interactions between adjacent molecules. On the other hand, Fig. 3**B** shows that the inclusion of DG-CDP in the formulation diminished the $1/C_s$ below 120 mN/m at the equilibrium π values of DPPC monolayers (30–35 mN/m).

The A_{molec} and the $1/C_s$ plotted in Fig. 3**C and 3D** as a function of the mole fraction of DG-CDP ($x_{DG\text{-}CDP}$) indicated that mixed DPPC/DG-CDP monolayers exhibited an ideal behavior, suggesting a homogeneous distribution of the components of the monolayer. To obtain stable Lip, with low polydispersity and suitable for drug delivery, higher $1/C_s$ would be required. In the case of neutral lipid films containing only zwitterionic molecules, this can be achieved by including small fractions of cholesterol in the formulation, as we have demonstrated in a previous article (García et al., 2021). However, in the case of mixed DPPC:DG-CDP monolayers in a mole ratio 7:3, as can be observed in Fig. 4**C**, it was necessary a mole fraction of cholesterol higher than 0.6 to reach $1/C_s$ higher than 100 mN/m at π values in the 30–35 mN/m range. In any case, we have tried to prepare DG-CDP-containing Lip with the lipidic composition indicated above, and we have found that the high fluidity of the lipidic films originated precipitates in the rehydration medium and the thin-film was hard to be redispersed. Therefore, to avoid fluidization

of the lipidic membrane induced by the interaction between the polar heads of DG-CDP, a very low concentration of nucleolipid was used ($x_{DG-CDP} = 0.03$) to prepare the Lip, maintaining the mechanical properties of the pure DPPC membrane. To slightly increase the rigidness of the film, a 0.03 mol ratio of cholesterol was added to the liposomal formulations.

In a previous work, the solubility of Dox in different media was studied to select the appropriate medium for drug loading through the transmembrane pH gradient method, from which ammonium sulfate solution was chosen, since it allowed the achievement of a high drug concentration within the Lip based on DPPC, DDAB and cholesterol (García et al., 2021). This method was also useful for encapsulating Dox inside the nucleolipid-based Lip. EE percentages higher than 80% (Table 1) were achieved, comparable to the Dox-containing liposomal formulations previously reported by the authors. Although the EE % were high, they were slightly lower than those of other reported Lip (Rehman et al., 2018; Zarchi et al., 2018), which can be explained due to differences in the composition of the bilayer (Abraham et al., 2005; Rehman et al., 2018). Furthermore, as shown in Table 1, Dox-loaded PEG-AuNPs-functionalized Lip exhibited slightly lower EE % compared to Lip-Dox. This effect on drug encapsulation has been previously reported for other Lip in which the presence of AuNPs decreased the drug loading efficiency (Zarchi et al., 2018). It has been argued that AuNPs can induce destabilization in the bilayer of Lip (Ghosh et al., 2008), which may facilitate leaking of part of encapsulated Dox from the aqueous compartment.

As expected, the surface functionalization with PEG-AuNPs not only affected the EE % but also the d_H and ζ values (Table 1). After anchoring, the size of liposomal dispersions, with and without Dox, increased almost 1.2-fold, and also the drug loading had an impact on the size of Lip. These results are in agreement with previous works in which higher d_H were observed as the system complexity was higher (Abraham et al., 2005; Rehman et al., 2018; Zarchi et al., 2018). All liposomal dispersions exhibited negative ζ values due to the negative charge of the phosphate groups of the nucleolipid DG-CDP (Prieto-Dapena et al., 2021b), which allowed surface functionalization with positively charged AuNPs. Therefore, the anchoring process induced a reduction in the absolute value of ζ when comparing non-decorated and PEG-AuNPs decorated Lip. This confirmed the electrostatic interaction between positively charged AuNPs and negatively charged Lip, as previously reported (Mady et al., 2012; Zarchi et al., 2018). Images obtained by FE-SEM analyses (Fig. 5) demonstrated the nearly spherical shapes of all Lip as well as their nano-scale sizes, comparable to those observed by DLS (García et al., 2021; Hou et al., 2020).

Liposomal formulations efficiently controlled the Dox release (Fig. 6) under different release conditions, acting as promising nanocarriers. As expected, Dox reference sample was released at a constant rate, independently of the medium and temperature, fitting to a Zero order model. Kinetic data results of both liposomal formulations fitted well to the Peppas model with *n* values near to 0.5 or the Higuchi model (Table 2), indicating a main Fickian transport in which the release of the drug was controlled by diffusion, in agreement with previous results (Haghiralsadat et al., 2018). Interestingly, they can trigger the drug release at acidic pH and hyperthermia temperature, confirming their responsiveness to both stimuli.

Release studies from PEG-AuNPs-functionalized Lip showed higher percentages of Dox released in both media (PBS pH 7.4 and ABS pH 5.1) and temperatures (37 °C and 42 °C) compared to Lip-Dox. Interestingly, the acidic medium and the high temperature had a higher impact on the Dox release from PEG-AuNPs-Lip-Dox than that from Lip-Dox, which demonstrated its usefulness as a pH-temperature dual-sensitive nucleolipid-containing stealth Lip.

The increase in the percentage of Dox release from both liposomal formulations at higher temperature (42 °C) compared to physiological temperature (37 °C) demonstrated their thermal response. This can be explained by considering that high temperatures enhance the fluidity of lipid membranes, leading to an increase in the permeability of the lipid bilayer and facilitating Dox diffusion (Jiang et al., 2011). This property is favored due to the presence of DPPC, since this zwitterionic lipid exhibits a phase transition temperature, around 41 °C (Naitlho et al., 2019). In the case of PEG-AuNPs-Lip-Dox, at high temperature, the formation of transient pores in the bilayer or other forms of mechanical disruption of the lipid bilayer may occur due to the AuNPs functionalization (Al-Ahmady et al., 2016). The responsiveness to temperature changes is particularly interesting in the treatment of cancer since tumor tissues usually show hyperthermia due to the rapid metabolism of cancer cells (Franco et al., 2021). Furthermore, PEG-AuNPs-functionalized Lip may also be used to be remotely activated by irradiation, triggering the drug release by light-induced heating response thanks to the presence of AuNPs (Hou et al., 2020; Lajunen et al., 2015; Li and Kataoka, 2020; Sau et al., 2009).

pH-responsive Lip can undergo phase transition and acquire fusogenic ability in acidic medium, leading to the cargo release. This property is of particular interest for anticancer drug delivery because the extracellular pH of cancer tissues is slightly acidic due to the high metabolic activity of cancer cells. This allows them to trigger drug release into the cytoplasm, optimizing cancer treatment (Aghdam et al., 2019; Franco et al., 2021; Rehman et al., 2018). If the components of Lip present acid-cleavable bonds or acid-base ionizable groups, responsiveness to pH changes can be obtained. The results showed that PEG-AuNPs-Lip-Dox exhibited pH-sensitive behavior when comparing the release profiles at 37 °C (Fig. 6**A and 6B**), while non-significant differences were observed in the release profiles from Lip-Dox. An explanation for this behavior may consider a change in the apparent pK_a of Dox ($pK_a1 = 7.34$ (phenol); $pK_a2 = 8.46$ (amine)) on the surface of AuNPs. A possible 1.2-fold reduction in the apparent pK_a of Dox can occur as a consequence of the high and positive ζ generated by the PEG-AuNPs (Tsui et al., 1986). This change in the apparent pK_a may produce neutral molecules of Dox capable of interacting either by specific adsorption on AuNPs (Curry et al., 2015) or by hydrogen bonds between the keto groups of Dox and the OH groups of the PEGylated AuNPs. Under acidic conditions (pH 5.1), Dox is protonated, inducing electrostatic repulsion with the AuNPs, then increasing its release.

The interaction of Dox with cytidine moiety of the nucleolipid and/or with the gold surface could have affected its activity by blocking the Dox release. However, cell viability studies carried out with human breast and ovarian cancer cell lines showed that Dox was released from the developed formulations (Lip-Dox and PEG-AuNPs-Lip-Dox) over time and that Dox preserved its cytotoxic activity against both cancer cells. Several authors have developed pH-temperature dual-responsive stealth Lip (Kanamala et al., 2019; Zhao et al., 2020; Zheng et al., 2017), but, to the best of our knowledge, this is the first report on DG-CDP-containing lipid vesicles functionalized with PEGylated-AuNPs for triggering delivery of Dox. Results in Fig. 7 suggest that both Dox-loaded Lip and AuNPs-Lip were released in a sustained manner over time, in agreement with the release results (Fig. 6). A short-time exposition to the liposomal formulations was insufficient to release enough Dox to the cancer cells and, therefore, they showed very low cytotoxicity. However, with an extension of the treatment time from 2 to 72 h, Lip-Dox and PEG-AuNPs-Lip-Dox showed high cytotoxic activity. As shown in the release studies, both Lip, with and without AuNPs surface anchoring, have been developed as stimuli-responsive nanocarriers, designed to release Dox in acidic environment and high temperature; however, cells were incubated in standard cell culture conditions (pH 7.4 and 37 °C) for the cell viability assay. As shown in Fig. 6**C**, PEG-AuNPs-Lip-Dox released almost 100% of Dox at pH 5.1 and 42 °C compared to approximately 65% at pH 7.4 and 37 °C. Thus, the lower cytotoxic effect of them compared to that of free Dox was probably due to the slower Dox release rate under cell culture conditions. In any case, these results show that PEG-AuNPs-Lip-Dox released Dox in a controlled manner without losing its anticancer effect. Further studies are required to evaluate the efficacy and safety of PEG-AuNPs-Lip-Dox, including studies under hyperthermia conditions and *in vivo* experiments in animal models of metastasis.

Although several pH-responsive (Tang et al., 2019) and thermo-responsive nanocarriers (Bordat et al., 2019), including polymer-based and lipid-based nanosysemts as carriers of Dox have been published hitherto and significant advances have been achieved in the development of Dox delivery systems (Zhao et al., 2018), to best of our knowledge, the here developed liposomal system is the first multifunctional nanoplatform that combines in a single nanocarrier i) a self-targeted component, the nucleolipid DG-CDP, ii) a dual pH/thermo-responsive behavior for triggered delivery of Dox, iii) a functionalized surface based on PEGylated-AuNPs that would allow preventing the immune system, being also useful for photothermal therapy. Even though different strategies have been explored to functionalize the surface of liposomal systems (Khan et al., 2020; Makwana et al., 2021), the as-described liposomal nanoplatform incorporates a nucleolipid, DG-CDP, as a key component of the Lip since it combines the self-assembly properties of the phospholipid structure and the specific recognition of the nucleoside fragment, which represents an important advance in the administration and targeting of nucleic acids. Moreover, DG-CDP provides negative surface charge, allowing surface functionalization with amine-terminated PEGylated-AuNPs, which plus DPPC, a zwitterionic lipid, lead to Lip with 'stealth' surfaces that would reduce protein binding and increase plasma residence time. Furthermore, variations in the pH and/or the temperature, specifically acidic media and hyperthermia conditions, may modify the fluidity and permeability of lipid bilayer, thus facilitating the triggered release of the drug allowing liposomal systems to behave as a stimuli-responsive nanocarrier; besides, the anchoring with AuNPs could be exploited for photothermal therapy with perspectives for cancer nanomedicine.

5. Conclusion

Summing up, our results indicated that DG-CDP can be used as scaffolding material of Lip and the developed nucleolipid-containing liposomal formulations would be a promising approach for cancer therapy because of their nano-scale size, stealth surface due to the anchored with PEGylated AuNPs, capacity to control the drug release under physiological conditions, triggering the Dox release under acidic and hyperthermia conditions, and anticancer activity. Overall, their promising properties could be further explored in other cancer cell lines as well as in murine models even in presence of an external stimulus for evaluating the light-induced heating response for hyperthermia therapy. In addition, studies to comprehensively analyze their efficacy and safety are also needed to better define their advantages over the traditional treatments with Dox or even other already reported Dox-loaded nanocarriers, mainly considering the side effects of Dox, viz., cardiotoxicity and damage on red blood cells.

CRediT authorship contribution statement

Mónica C. García: Conceptualization, Methodology, Validation, Formal analysis, Investigation, Writing – original draft, Writing – review & editing, Project administration, Funding acquisition. **José Manuel Calderón-Montaño:** Methodology, Formal analysis, Investigation, Writing – original draft, Writing – review & editing. **Manuela Rueda:** Investigation, Resources, Writing – review & editing, Funding acquisition. **Marcela Longhi:** Investigation, Writing – review & editing. **Antonio M. Rabasco:** Conceptualization, Investigation, Resources, Funding acquisition. **Miguel López-Lázaro:** Investigation, Resources, Writing – review & editing, Funding acquisition. **Francisco Prieto-Dapena:** Conceptualization, Validation, Investigation, Resources, Writing – original draft, Writing – review & editing, Supervision, Funding acquisition. **María Luisa González-Rodríguez:** Conceptualization, Validation, Investigation, Resources, Writing – review & editing, Supervision, Project administration, Funding acquisition.

Declaration of Competing Interest

The authors declare that they have no known competing financial interests or personal relationships that could have appeared to influence the work reported in this paper.

Acknowledgments

García MC and Longhi M are members of Argentinean National Council for Scientific and Technical Research (CONICET)'s scientific career. The authors wish to acknowledge the assistance of the CONICET and the National University of Cordoba (UNC, Argentina), both of which provided facilities for this work. Furthermore, García MC thanks AUIP for the fellowship awarded to conduct a research visit in the Faculty of Pharmacy, Universidad de Sevilla. The authors also acknowledge the assistance of CITIUS at the Universidad de Sevilla for providing facilities for this work, and especially wish to thank technicians Cristina Vaquero y Francisco Varela for their optimal technical assistance in FE-SEM.

Funding sources

This research was funded by the Ministry of Science and Innovation of Spain (Grant number CTQ2014-57515-C2-1), the Junta de Andalucía (Grant numbers FQM202 and CTS214), the CITIUS Services, the VI Plan Propio of the Universidad de Sevilla, the Agencia Nacional de Promoción Científica y Tecnológica – Fondo para la investigación Científica y Tecnológica (Grant number FonCyT-PICT 2019-00048) and the Secretaría de Ciencia y Tecnología, Universidad Nacional de Córdoba (SeCyT-Formar Grant number 33820190100091CB).

References

Abraham, S.A., Waterhouse, D.N., Mayer, L.D., Cullis, P.R., Madden, T.D., Bally, M.B., 2005. The liposomal formulation of doxorubicin. Methods Enzymol. 71–97. Elsevier.
Aghdam, M.A., Bagheri, R., Mosafer, J., Baradaran, B., Hashemzaei, M., Baghbanzadeh, A., de la Guardia, M., Mokhtarzadeh, A., 2019. Recent advances on thermosensitive and pH-sensitive liposomes employed in controlled release. J. Control. Release 315, 1–22.
Al-Ahmady, Z., Lozano, N., Mei, K.-C., Al-Jamal, W.T., Kostarelos, K., 2016. Engineering thermosensitive liposome-nanoparticle hybrids loaded with doxorubicin for heat-triggered drug release. Int. J. Pharm. 514 (1), 133–141.
Allain, V., Bourgaux, C., Couvreur, P., 2012. Self-assembled nucleolipids: from supramolecular structure to soft nucleic acid and drug delivery devices. Nucleic Acids Res. 40 (5), 1891–1903.
Alvarez-Malmagro, J., Su, ZhangFei, Leitch, J.J., Prieto, F., Rueda, M., Lipkowski, J., 2019. Electric-field-driven molecular recognition reactions of guanine with 1, 2-dipalmitoyl-sn-glycero-3-cytidine monolayers deposited on gold electrodes. Langmuir 35 (28), 9297–9307.
Alvarez-Malmagro, J., Su, ZhangFei, Leitch, J.J., Prieto, F., Rueda, M., Lipkowski, J., 2020. Molecular recognition between guanine and cytosine-functionalized nucleolipid hybrid bilayers supported on gold (111) electrodes. Bioelectrochemistry 132.
Argudo, P.G., Muñoz, E., Giner-Casares, J.J., Martín-Romero, M.T., Camacho, L., 2019. Folding of cytosine-based nucleolipid monolayer by guanine recognition at the air-water interface. J. Colloid Interface Sci. 537, 694–703.
Bangham, A.D., Horne, R.W., 1964. Negative staining of phospholipids and their structural modification by surface-active agents as observed in the electron microscope. J. Mol. Biol. 8 (5), 660–IN10.
Barthélemy, P., 2009. Nucleoside-based lipids at work: From supramolecular assemblies to biological applications. C. R. Chim. 12 (1-2), 171–179.
Beltrán-Gracia, E., López-Camacho, A., Higuera-Ciapara, I., Velázquez-Fernández, J.B., Vallejo-Cardona, A.A., 2019. Nanomedicine review: clinical developments in liposomal applications. Cancer Nanotechnol. 10, 1–40.
Boedtkjer, E., Pedersen, S.F., 2020. The acidic tumor microenvironment as a driver of cancer. Annu. Rev. Physiol. 82 (1), 103–126.
Bordat, A., Boissenot, T., Nicolas, J., Tsapis, N., 2019. Thermoresponsive polymer nanocarriers for biomedical applications. Adv. Drug Deliv. Rev. 138, 167–192.
Cai, F., Luis, M.A.F., Lin, X., Wang, M., Cai, L., Cen, C., Biskup, E., 2019. Anthracycline-induced cardiotoxicity in the chemotherapy treatment of breast cancer: Preventive strategies and treatment. Mol. Clin. Oncol. 11, 15–23.
Costa, P., Lobo, J.M.S., 2001. Modeling and comparison of dissolution profiles. Eur. J. Pharmaceut. Sci. 13 (2), 123–133.
Curry, D., Cameron, A., MacDonald, B., Nganou, C., Scheller, H., Marsh, J., Beale, S., Lu, M., Shan, Z., Kaliaperumal, R., Xu, H., Servos, M., Bennett, C., MacQuarrie, S., Oakes, K.D., Mkandawire, M., Zhang, X.u., 2015. Adsorption of doxorubicin on

citrate-capped gold nanoparticles: insights into engineering potent chemotherapeutic delivery systems. Nanoscale 7 (46), 19611–19619.
Douedi, S., Carson, M.P., 2019. Anthracycline medications (Doxorubicin). In: StatPearls [Internet]. Treasure Island (FL): StatPearls Publishing.
Franco, M.S., Gomes, E.R., Roque, M.C., Oliveira, M.C., 2021. Triggered Drug Release From Liposomes: Exploiting the Outer and Inner Tumor Environment. Front. Oncol. 11, 470.
García, M.C., 2019. Nano-and microparticles as drug carriers, Engineering Drug Delivery Systems. Elsevier, Cambridge, UK, pp. 71–110. https://www.sciencedirect.com/science/article/pii/B9780081025482000044.
García, M.C., Aloisio, C., Onnainty, R., Ullio-Gamboa, G., 2017. Self assembled nanomaterials. In: Narayan, R. (Ed.), Nanobiomaterials: Nanostructured materials for biomedical applications, first ed. Woodhead Publishing, Cambridge, UK, pp. 41–94. https://www.sciencedirect.com/science/article/pii/B9780081007167000039.
García, M.C., Naitlho, N., Calderón-Montaño, J.M., Drago, E., Rueda, M., Longhi, M., Rabasco, A.M., López-Lázaro, M., Prieto-Dapena, F., González-Rodríguez, M.L., 2021. Cholesterol levels affect the performance of AuNPs-decorated thermo-sensitive liposomes as nanocarriers for controlled doxorubicin delivery. Pharmaceutics 13, 973.
García, M.C., Uberman, P., 2019. Nanohybrid fillers-based drug delivery systems. In: Shyam, M., Shivendu, R., Nandita, D., Raghvendra, M., Sabu, T. (Eds.), Nanocarriers for drug delivery. Nanoscience and Nanotechnology in Drug Delivery, first ed. Woodhead Publishing, Cambridge, UK, pp. 43–79. https://www.sciencedirect.com/science/article/pii/B9780128140338000023.
Ghosh, P., Han, G., De, M., Kim, C.K., Rotello, V.M., 2008. Gold nanoparticles in delivery applications. Adv. Drug Deliv. Rev. 60, 1307–1315.
Haghiralsadat, F., Amoabediny, G., Helder, M.N., Naderinezhad, S., Sheikhha, M.H., Forouzanfar, T., Zandieh-Doulabi, B., 2018. A comprehensive mathematical model of drug release kinetics from nano-liposomes, derived from optimization studies of cationic PEGylated liposomal doxorubicin formulations for drug-gene delivery. Artif. Cells Nanomed. Biotechnol. 46, 169–177.
Hou, K., Bao, M., Xin, C., Wang, L., Zhang, H., Zhao, H., Wang, Z., 2020. Green synthesis of gold nanoparticles coated doxorubicin liposomes using procyanidins for light–controlled drug release. Adv. Powder Technol. 31, 3640–3649.
Jain, A., Jain, S.K., 2016. In vitro release kinetics model fitting of liposomes: an insight. Chem. Phys. Lipids 201, 28–40.
Jiang, W., Lionberger, R., Yu, L.X., 2011. In vitro and in vivo characterizations of PEGylated liposomal doxorubicin. Bioanalysis 3, 333–344.
Kanamala, M., Palmer, B.D., Jamieson, S.M.F., Wilson, W.R., Wu, Z., 2019. Dual pH-sensitive liposomes with low pH-triggered sheddable PEG for enhanced tumor-targeted drug delivery. Nanomedicine 14, 1971–1989.
Khan, A.A., Allemailem, K.S., Almatroodi, S.A., Almatroudi, A., Rahmani, A.H., 2020. Recent strategies towards the surface modification of liposomes: an innovative approach for different clinical applications. 3. Biotech 10, 1–15.
Koltai, T., 2020. The pH paradigm in cancer. Eur. J. Clin. Nutr. 74, 14–19.
Lajunen, T., Viitala, L., Kontturi, L.-S., Laaksonen, T., Liang, H., Vuorimaa-Laukkanen, E., Viitala, T., Le Guével, X., Yliperttula, M., Murtomäki, L., 2015. Light induced cytosolic drug delivery from liposomes with gold nanoparticles. J. Control. Release 203, 85–98.
Large, D.E., Abdelmessih, R.G., Fink, E., Auguste, D.T., 2021. Liposome composition in drug delivery design, synthesis, characterization, and clinical application. Adv. Drug Deliv. Rev. 113851.
Li, J., Kataoka, K., 2020. Chemo-physical Strategies to Advance the in Vivo Functionality of Targeted Nanomedicine: The Next Generation. J. Am. Chem. Soc.
Li, Y., Angelova, A., Hu, F., Garamus, V.M., Peng, C., Li, N., Liu, J., Liu, D., Zou, A., 2019. pH responsiveness of hexosomes and cubosomes for combined delivery of Brucea javanica oil and doxorubicin. Langmuir 35, 14532–14542.
Loew, M., Springer, R., Scolari, S., Altenbrunn, F., Seitz, O., Liebscher, J.R., Huster, D., Herrmann, A., Arbuzova, A., 2010. Lipid domain specific recruitment of lipophilic nucleic acids: a key for switchable functionalization of membranes. J. Am. Chem. Soc. 132, 16066–16072.
Lozano, N., Al-Jamal, W.T., Taruttis, A., Beziere, N., Burton, N.C., Van den Bossche, J., Mazza, M., Herzog, E., Ntziachristos, V., Kostarelos, K., 2012. Liposome–gold nanorod hybrids for high-resolution visualization deep in tissues. J. Am. Chem. Soc. 134, 13256–13258.
Lyon, P.C., Gray, M.D., Mannaris, C., Folkes, L.K., Stratford, M., Campo, L., Chung, D.Y. F., Scott, S., Anderson, M., Goldin, R., 2018. Safety and feasibility of ultrasound-triggered targeted drug delivery of doxorubicin from thermosensitive liposomes in liver tumours (TARDOX): a single-centre, open-label, phase 1 trial. Lancet Oncol. 19, 1027–1039.
Mady, M.M., Fathy, M.M., Youssef, T., Khalil, W.M., 2012. Biophysical characterization of gold nanoparticles-loaded liposomes. Physica Med. 28, 288–295.
Makwana, V., Karanjia, J., Haselhorst, T., Anoopkumar-Dukie, S., Rudrawar, S., 2021. Liposomal doxorubicin as targeted delivery platform: Current trends in surface functionalization. Int. J. Pharm. 593, 120117.
Michanek, A., Yanez, M., Wacklin, H., Hughes, A., Nylander, T., Sparr, E., 2012. RNA and DNA association to zwitterionic and charged monolayers at the air–liquid interface. Langmuir 28, 9621–9633.
Milczewska, K., Voelkel, A., Zwolińska, J., Jędro, D., 2016. Preparation of hybrid materials for controlled drug release. Drug Dev. Ind. Pharm. 42, 1058–1065.
Montanha, E.A., Caseli, L., Kaczmarek, O., Liebscher, J., Huster, D., Oliveira Jr, O.N., 2011. Comparative study of liponucleosides in Langmuir monolayers as cell membrane models. Biophys. Chem. 153, 154–158.
Montis, C., Milani, S., Berti, D., Baglioni, P., 2012. Complexes of nucleolipid liposomes with single-stranded and double-stranded nucleic acids. J. Colloid Interface Sci. 373, 57–68.
Montizaan, D., Yang, K., Reker-Smit, C., Salvati, A., 2020. Comparison of the uptake mechanisms of zwitterionic and negatively charged liposomes by HeLa cells. Nanomed. Nanotechnol. Biol. Med. 30, 102300.
Naitlho, N., Prieto-Dapena, F., Rabasco, A.M., Rueda, M., González-Rodríguez, M.L., 2019. Didodecyldimethylammonium bromide role in anchoring gold nanoparticles onto liposome surface for triggering the drug release. AAPS PharmSciTech 20, 1–13.
National Cancer Institute, 2020. Doxorubicin Hydrochloride. In: NIH Turning.
Oumzil, K., Khiati, S., Camplo, M., Koquely, M., Chuttani, K., Chaturvedi, S., Mishra, A. K., Barthélémy, P., 2014. Nucleolipids as building blocks for the synthesis of 99m Tc-labeled nanoparticles functionalized with folic acid. New J. Chem. 38, 5240–5246.
Park, S.M., Kim, M.S., Park, S.J., Park, E.S., Choi, K.S., Kim, Y.S., Kim, H.R., 2013. Novel temperature-triggered liposome with high stability: formulation, in vitro evaluation, and in vivo study combined with high-intensity focused ultrasound (HIFU). J. Control. Release 170, 373–379.
Pokholenko, O., Gissot, A., Vialet, B., Bathany, K., Thiéry, A., Barthélémy, P., 2013. Lipid oligonucleotide conjugates as responsive nanomaterials for drug delivery. J. Mater. Chem. B 1, 5329–5334.
Prieto-Dapena, F., Su, Z., Alvarez-Malmagro, J., Rueda, M., Lipkowski, J., 2021a. Electrostatics affects formation of Watson-Crick complex between DNA bases in monolayers of nucleolipids deposited at a gold electrode surface. Electrochim. Acta 138816.
Prieto-Dapena, F., Su, Z., Alvarez-Malmagro, J., Rueda, M., Lipkowski, J., 2021b. Mixed monolayer of a nucleolipid and a phospholipid has improved properties for spectroelectrochemical sensing of complementary nucleobases. J. Electroanal. Chem. 896, 115120.
Ramzy, L., Nasr, M., Metwally, A.A., Awad, G.A.S., 2017. Cancer nanotheranostics: a review of the role of conjugated ligands for overexpressed receptors. Eur. J. Pharm. Sci. 104, 273–292.
Rehman, A.U., Omran, Z., Anton, H., Mély, Y., Akram, S., Vandamme, T.F., Anton, N., 2018. Development of doxorubicin hydrochloride loaded pH-sensitive liposomes: Investigation on the impact of chemical nature of lipids and liposome composition on pH-sensitivity. Eur. J. Pharm. Biopharm. 133, 331–338.
Rouquette, M., Lepetre-Mouelhi, S., Couvreur, P., 2019. Adenosine and lipids: A forced marriage or a love match? Adv. Drug Deliv. Rev. 151, 233–244.
Sau, T.K., Urban, A.S., Dondapati, S.K., Fedoruk, M., Horton, M.R., Rogach, A.L., Stefani, F.D., Rädler, J.O., Feldmann, J., 2009. Controlling loading and optical properties of gold nanoparticles on liposome membranes. Colloids and Surf. A: Physicochem. Eng. Aspects 342, 92–96.
Sritharan, S., Sivalingam, N., 2021. A comprehensive review on time-tested anticancer drug doxorubicin. Life Sci. 119527.
Tang, H., Zhao, W., Yu, J., Li, Y., Zhao, C., 2019. Recent development of pH-responsive polymers for cancer nanomedicine. Molecules 24, 4.
Thorn, C.F., Oshiro, C., Marsh, S., Hernandez-Boussard, T., McLeod, H., Klein, T.E., Altman, R.B., 2011. Doxorubicin pathways: pharmacodynamics and adverse effects. Pharmacogenet. Genomics 21, 440.
Torres, J., Dhas, N., Longhi, M., García, M.C., 2020. Overcoming Biological Barriers With Block Copolymers-Based Self-Assembled Nanocarriers. Recent Advances in Delivery of Anticancer Therapeutics. Front. Pharmacol. 11, 1840.
Tsui, F.C., Ojcius, D.M., Hubbell, W.L., 1986. The intrinsic pKa values for phosphatidylserine and phosphatidylethanolamine in phosphatidylcholine host bilayers. Biophys. J. 49, 459–468.
U.S. Pharmacopoeial Convention, 2015. United States Pharmacopoeia (38). The National Formulary and Dispensing Information (33) United States Pharmacopeia Convention Inc., Rockville, Maryland.
Xin, Y., Kong, X., Zhang, X., Lv, Z., Du, X., 2012. Self-assembly and molecular recognition of adenine-and thymine-functionalized nucleolipids in the mixed monolayers and thymine-functionalized nucleolipids on aqueous melamine at the air–water interface. Langmuir 28, 11153–11163.
Zarchi, A.A.K., Amini, S.M., Salimi, A., Kharazi, S., 2018. Synthesis and characterisation of liposomal doxorubicin with loaded gold nanoparticles. IET Nanobiotechnol. 12, 846–849.
Zhao, N., Woodle, M.C., Mixson, A.J., 2018. Advances in delivery systems for doxorubicin. J. Nanomed. Nanotechnol. 9.
Zhao, Y., Cai, F., Shen, X., Su, H., 2020. A high stable pH-temperature dual-sensitive liposome for tuning anticancer drug release. Synth. Syst. Biotechnol. 5, 103–110.
Zheng, Y., Wang, L., Lu, L., Wang, Q., Benicewicz, B.C., 2017. pH and thermal dual-responsive nanoparticles for controlled drug delivery with high loading content. ACS Omega 2, 3399–3405.